LHC BEAM VACUUM EVOLUTION DURING 2015 MACHINE OPERATION

C. Yin Vallgren*, G. Bregliozzi, P. Chiggiato
CERN, Geneva, Switzerland

Abstract

The LHC successfully returned to operation in April, 2015 after almost 2 years of Long Shutdown 1 (LS1) for various upgrade and consolidation programs. During 2015 operation, the LHC operated for more than 1000 fills. The 2015 LHC proton physics ended with 2244 bunches per beam circulating with 25 ns bunch spacing at top energy of 6.5 TeV. This paper summarizes the dynamic vacuum observations in different locations along the LHC during dedicated fills as well as during physics runs with both 50 ns and 25 ns bunch spacing. The causes for the dynamic pressure rises are investigated and are presented. A clear beam conditioning effect is observed, as well as a so-called deconditioning effect. Furthermore, for the experimental areas, the dynamic pressure evolution is also presented.

LHC BEAM OVERVIEW

The overview of the LHC beam schedule along the year is summarized in Fig. 1. In 2015, the LHC operated for more than 1000 fills. The 2015 LHC proton physics started with beam of low intensity at 6.5 TeV, followed by two scrubbing runs of high intensity beams at 450 GeV for about 3 weeks, finally ended with 2244 bunches per beam circulating with 25 ns bunch spacing at top energy of 6.5 TeV. The last month of the LHC physics run in 2015 was dedicated to lead ions.

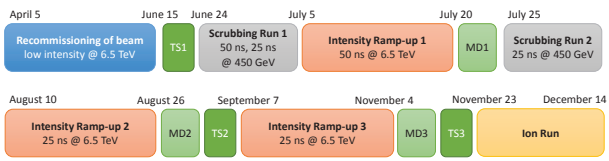

Figure 1: LHC beam schedule 2015. TS: technical stop; MD: machine development.

LHC LONG STRAIGHT SECTION PRESSURE EVOLUTION OVERVIEW

In this section, an overview of the average dynamic pressure rise for several specific locations at room temperature in the LHC Long Straight Sections (LSS) with physics beam of 25 ns at 6.5 TeV during the 2015 operation is presented.

In Fig. 2, the plotted value is the normalized maximum of the average dynamic pressure rise taken in each selected fill. The shown pressure readings were measured by Bayard Alpert gauges which are located (±100-120 m from the interaction point) in the combination chambers (CC) of each LSS, where both beams circulate at the same time and are mostly NEG coated. Because of the two beams coming from both directions, the effective bunch spacing in these regions can be as low as half of 25 ns. As seen in Fig. 2, with less than 800 bunches, the dynamic pressure rise in the common beam pipes is almost negligible in all of the LSSs, which is also a clear proof for the electron cloud mitigation effect of the NEG coating (activated NEG has an SEY of 1.1). While increasing the total bunch numbers injected in the LHC, in all the LSSs along the LHC, an average improvement of a factor 5 in the normalized pressure was observed due to accumulated scrubbing effect by the proton beams during the physics runs. LSS1 (accommodating ATLAS) and LSS5 (accommodating CMS) generally seem to have much better pressure (a factor 10 lower) compared to the other long straight sections, LSS2 (ALICE) and LSS8 (LHCb) in the LHC. The explanation for a higher background in the LSS2 and LSS8 is mainly due to the contribution of the high dynamic pressure rise in the injection areas due to the target dump for the injection (TDI2, TDI8) and the magnet kickers' for the injection (MKIs).

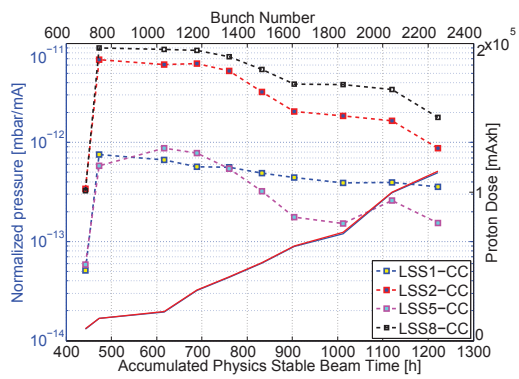

Figure 2: The dynamic pressure increase in the LHC long straight sections along 2015 physics run, as a function of accumulated beam time and increased bunch number.

Figure 3 gives a comparison between the pressure in the transition between two NEG coated beam pipes in the baked and activated vacuum system and the pressure in cold-warm transition in the un-baked and cryo-system. Significant improvement is visible in pressure for both the NEG coated transition and the cryo-system. As seen in Fig. 3, the pressure rise in the C-W transition with synchrotron radiation is about 4 times higher than the one without.

* christina.yin.vallgren@cern.ch

ISBN 978-3-95450-147-2

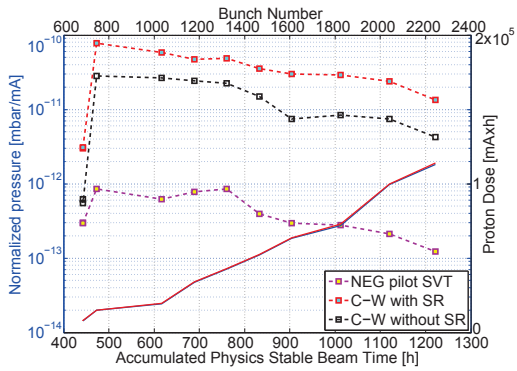

Figure 3: Comparison between normalized pressure rise in the NEG-NEG transition pf the baked and activated vacuum system and the cold-warm transition in the un-baked and cryo-system.

LHC ARC PRESSURE OVERVIEW

Average of the dynamic pressure and the measured heat load in the different arcs versus number of bunches are shown in Fig. 4. Scrubbing runs provided sufficient mitigation against beam-induced pressure rise at 450 GeV but full suppression of the electron cloud was not achieved due to the difficulty with the beam instability. During the 2015 physics run with 1450b (1.5×10^{14} p, with 144b trains) the cooling capacity on the arc beam screen started approaching its design limit (160 W/half cell). A standard half cell in the ARC consists of three 15 m dipoles and 1 quadrupole with a total length of 53.45 m [1]. By the end of the proton run, 2244b was reached by using trains of 36b with 1.2×10^{11} p/b. The heat load per bunch significantly decreased during the physics run by using the filling scheme with short bunch trains due to the fact that less electron cloud was produced. The heat load in ARCs 12, 23 and 78 are close to the limit. The same pattern could not be found in the pressure evolution. In term of pressure, the sector with highest pressure rise is ARC 34 (in Fig. 4(a)), which is in reverse to the fact that ARC 34 gives the lowest heat load, as shown in Fig. 4(b). From the summary of pressure and heat load shown here, no correlation between pressure and heat load can be seen.

During the 2015 operation, loss of conditioning has been observed. After the technical stops and low intensity run, a clear increase in pressure rise was observed, as presented in Fig. 5. The pressure conditioning seemed to be partially reset on the Cu surfaces in the beam screens of the ARCs. The loss of conditioning seemed to be much stronger after low intensity beams than long term in-activities of beam. Scrubbing effect seemed to be reasonably well preserved during short technical stops. The same pattern is also found with the bunch power loss measurements presented in [2]. This behavior of de-conditioning needs further investigation.

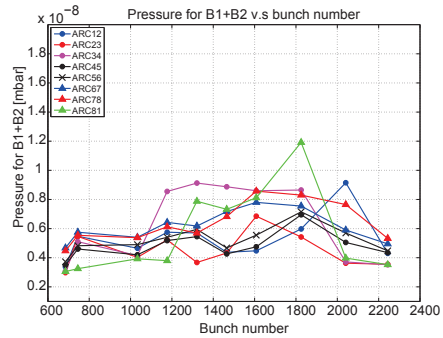

(a)

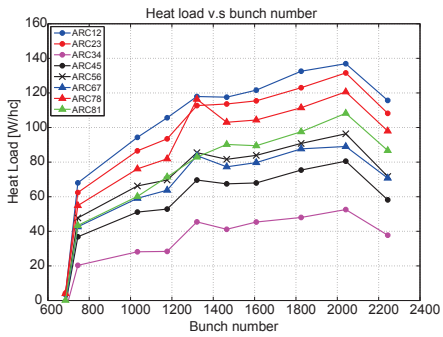

(b)

Figure 4: Average pressure reading for both B1 and B2 (a) and heat load (b) for each ARC versus bunch number for selected fills.

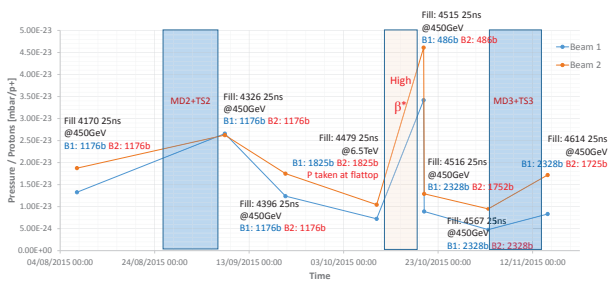

Figure 5: Observed de-conditioning effect in pressure in the LHC ARCs during the technical stops and the high β^* run. Average maximum pressure of each of the ARCs for the selected scrubbing validation fills at 450 GeV.

LHC EXPERIMENT PRESSURE OVERVIEW

Figure 6 shows the average dynamic pressure rise in each of the experimental areas with beam of 25 ns at 6.5 TeV during the 2015 operation, at the flat-top. For all experiments apart from CMS, no increase of pressure is seen with increasing bunch numbers. For the CMS experimental area, the pressure increased for the last two selected fills with high intensity beams is due to the solenoid of the detector switched-off. The detector solenoid, which changes the longitudinal motion of the electrons [3] has a known effect in the electron cloud reduction, which gives a direct

impact in pressure in all the experimental areas. Figure 8 shows two pressure plots for the two selected fills in the CMS. The main difference between the two selected fills is one with the CMS detector solenoid on and the other without. A clear difference in the pressure induced by electron cloud is seen, when the beams were injected. It is also noted that the CMS gauges seem to be very sensitive to electronics interference.

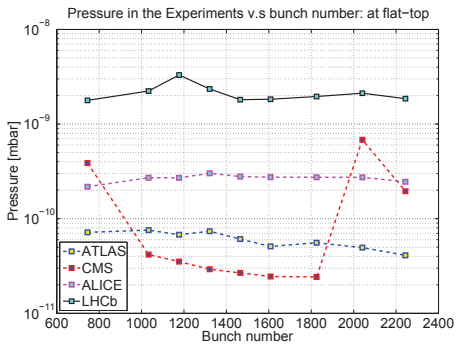

Figure 6: The maximum of average dynamic pressure as a function of bunch number in the LHC experiment areas in each selected fill at flat top. The same selected fills are used as for LSSs and ARCs.

Dynamic pressure as a function of time for a typical physics fill, for example, in ATLAS and CMS is plotted for each experiment and shown in Fig. 7 and 8(a). A clear correlation between the dynamic pressure and the beam intensity, beam energies and luminosity is shown. The typical behavior in pressure can be divided into three main pressure rises, with a typical example of ATLAS detailed in Fig. 7. The first pressure increase with maximum at the end of injection is due to electron cloud development in the beam pipe. The second increase with maximum at the end of the beam energy ramp-up is due to desorption induced by synchrotron radiation from the inner-triplets. The third one well correlates with the luminosity; the same is measured in CMS (Fig. 8(a)). However, the reason for the sudden pressure rise right after the collision is yet unclear. This could be a result of collision debris desorbing gas from the walls of the beam pipe. Or this could also be interference of electronics in the cables for the gauges close to the interaction point area. However, it is worth to mention that the pressure seems to increase with increasing luminosity. More studies in this area in order to gain a deeper understanding of the origin of pressure rise after the collision are ongoing and dedicated tests will take place during 2016 beam operation. The same analysis has been done for ALICE and LHCb. Since the collision rate for ALICE and LHCb is comparably small, no visible pressure rise is detected in collisions and only pressure rise due to electron cloud and synchrotron radiation are observed.

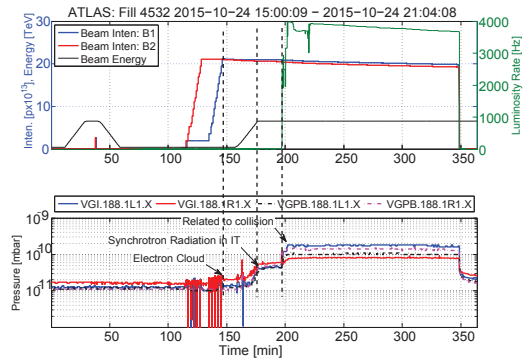

Figure 7: ATLAS: Fill 4532 1825b (2×72 bunch trains).

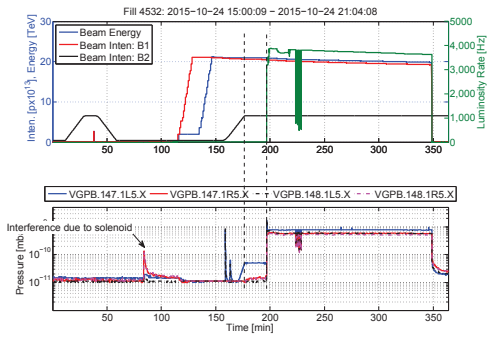

(a)

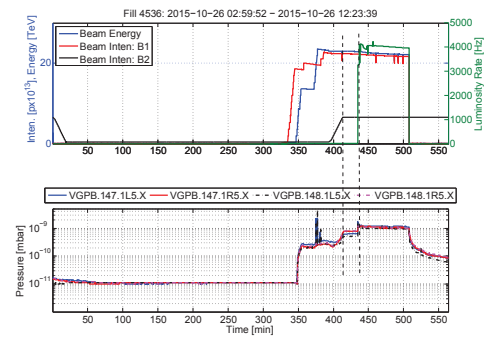

(b)

Figure 8: CMS: (a) Fill 4532 (1825b with 2×72 bunch trains): CMS detector solenoid on. (b) Fill 4536 (2041 with 2×72 bunch trains): CMS detector solenoid off.

REFERENCES

[1] Chapter 11, Cryogenic in LHC Design Report.

[2] G. Iadarola, et al, Chamonix 2016

[3] F. Zimmermann, Chamonix XI 2000

ISBN 978-3-95450-147-2